Chemical Vapor Deposition Repair of Graphene Oxide: A Route to Highly Conductive Graphene Monolayers

By *Vicente López, Ravi S. Sundaram, Cristina Gómez-Navarro,* David Olea, Marko Burghard, Julio Gómez-Herrero, Félix Zamora,* and *Klaus Kern*

High-quality graphene, owing to its extremely high carrier mobility,[1,2] has emerged as a promising component for nanoscale electrical devices.[3] So far, the fabrication of graphene-based devices has largely relied upon mechanical exfoliation of graphite.[4] However, this method yields only a small number of graphene monolayers, which have to be located in a time-demanding process. An alternative method – epitaxial growth of graphene on silicon carbide[5] – affords high-quality mono- and multi-layers of graphene, but the ultrahigh vacuum required limits its technological applicability. Another route involves chemical vapor deposition (CVD) of hydrocarbons on the surfaces of transition metals, like nickel, with subsequent sheet transfer onto insulating substrates,[6] yielding graphene devices of promising electrical performance. However, the sheets obtained in this manner still lack sufficient structural homogeneity over larger areas. Furthermore, as a general disadvantage of all the aforementioned methods, they do not enable the controlled placement of the graphene, which represents an essential prerequisite for the fabrication of integrated device architectures.

For these reasons, significant effort has recently been directed toward solution-based approaches that provide access to larger amounts of graphene monolayers, and furthermore offer the possibility of assembling the sheets at specific, surface-modified areas on a technologically relevant insulating substrate, such as SiO_2.[7]

High-quality graphene sheets have been obtained via ultrasonic dispersion of graphite in appropriate organic solvents.[8,9] However, this has been achieved only with lateral sizes of a few hundreds of nanometers,[8] and at quite low yield.[9] A very promising low-cost, up-scalable synthetic approach comprises the reduction of graphene oxide (GO) sheets,[10] which can be deposited with controllable density onto a wide range of substrates. Chemical reduction converts the close-to-insulating GO into sheets with up to four orders of magnitude higher electrical conductivity.[11–13] Such chemically derived graphene is a versatile basis for fabricating thin conductive films on solid supports,[14,15] thus opening access to transparent flexible electrodes.[15–17] For the electrical conductivity of monolayers of reduced GO, only moderate values, of 0.1–50 S cm^{-1}, have been found, which has been attributed to the presence of defects or residual functional groups remaining after reduction.[11–13] Strategies to heal these defects are thus needed for more demanding device applications. Here, we demonstrate that this task can be approached by a CVD process that enables the substitution of carbon atoms contained within the defective areas. In this manner, chemically derived graphene sheets of large dimension and with two orders of magnitude enhanced conductivity, compared to the merely reduced GO, can be obtained.

Our process starts by oxidizing graphite flakes of 20 μm size (Sigma Aldrich) using the Hummers method.[18] The oxidation product is then dispersed with the aid of mild sonication in water, followed by deposition of the resulting GO sheets onto degenerately doped silicon substrates covered by a thermally grown SiO_2 layer (300 nm thickness). According to atomic force microscopy (AFM) analysis, more than 90% of the objects are single layers, with a height of ~1 nm and lateral sizes ranging from several hundreds of nanometers to 10 μm. Substrate coverage can be adjusted by controlling the time of deposition and solution concentration. In this work, samples with approximately 30% coverage are introduced in a quartz tube furnace and subjected to a flow of mixture comprising 1 500 sccm of H_2 and 200 sccm of Ar for 20 min at 500 °C. The two-probe electrical conductivity of the hydrogen-treated sheets was found to range between 0.1 and 2 S cm^{-1} at room temperature, in close correspondence to the values observed after GO reduction by hydrazine or hydrogen plasma.[11] Increasing the reduction temperature to 900 °C or the reaction time up to 60 min provided very similar results. This finding suggests, as will be discussed below, that the electrical conductivity is limited by the presence of defects in the form of carbon vacancie, which cannot be healed by annealing or reduction.

The subsequent CVD step, which turned out to be crucial for obtaining improved conductivity, is performed after reduction in the same furnace. The CVD is carried out using ethylene as a carbon source, under conditions (2 sccm ethylene for 3 min at 800 °C) that are very similar to those in the CVD synthesis of

---

[*] Dr. C. Gómez-Navarro, Dr. D. Olea, Prof. J. Gómez-Herrero
Departamento de Física de la Materia Condensada
Universidad Autónoma de Madrid
28049 Madrid (Spain)
E-mail: cristina.gomez@uam.es

Dr. V. López, Dr. F. Zamora
Departamento de Química Inorgánica
Universidad Autónoma de Madrid
28049 Madrid (Spain)

R. S. Sundaram, Dr. C. Gómez-Navarro, Dr. M. Burghard, Prof. K. Kern
Max-Planck-Institut für Festkörperforschung
Heisenbergstrasse 1, 70569 Stuttgart (Germany)

Prof. K. Kern
Ecole Polytechnique Fédérale de Lausanne
1015 Lausanne (Switzerland)

DOI: 10.1002/adma.200901582

single-wall carbon nanotubes on SiO_2 substrates,[19] except for the presence of metal catalysts in the latter case. AFM imaging of the same monolayers before and after the two-step process showed no detectable height and lateral increase within the resolution of the AFM. The resulting monolayers (CVDGO) exhibited room-temperature conductivities in the range of 10–350 S cm^{-1}, corresponding to an average increase in conductivity of two orders of magnitude over the merely reduced sheets (see Fig. 1). The CVD step proved to be quite insensitive to variations in the flux rate (1–6 sccm) and deposition time (1–6 min), whereas a critical dependence on temperature was observed (optimum value ~800 °C). Lower temperatures resulted in samples with unaltered conductivity, while higher temperatures led to complete degradation of the reduced GO layers. Four-probe electrical measurements on CVDGO monolayers indicate that contact resistances make a measurable but minor contribution to the overall resistance of the AuPd-contacted monolayers. As a representative example, the sheet shown in Fig. 2a displays a total resistance of 14 kΩ and a contact resistance of 4 kΩ. The latter value is in agreement with the extrapolation from the corresponding dependence of resistance on contacted length (Fig. 2b). At the same time, the linear dependence of the plot rules out ballistic transport through these devices. Moreover, low-temperature four-probe measurements revealed that the contact resistance does not become dominant even at low temperatures.

Electrical studies were also performed in field-effect transistor (FET) configuration, with the degenerately doped silicon wafer utilized as back gate (Fig. 2c). From the acquired transfer characteristics, room-temperature field-effect hole mobilities between 1 and 50 $cm^2 V^{-1} s^{-1}$ were extracted for CVDGO (corresponding to a more than 50-fold increase over the reduced GO). For all CVDGO samples, even when measured under an He atmosphere, a pronounced shift of the current minimum (Dirac point) toward positive gate voltage was observed. Such persistent p-type doping is in contrast to the behavior of mechanically exfoliated graphene, in which the Dirac point moves closely to $V_{gate} = 0$ V upon oxygen removal.[20] Significant p-type doping has also been observed in other GO-derived graphene samples, and attributed to the presence of positively charged species screening the gate-induced electric field.[21] It is worth mentioning that this unintentional doping is also responsible for the slightly different enhancement factors observed for conductivity and mobility, since conductivity is always calculated at $V_g = 0$ V.

Despite the improved conductivity of the samples, evidence for a significant number of defects in the CVDGO was gained from Raman spectra, which exhibit a very intense D-line at ~1 350 cm^{-1} in addition to the G-line below 1 600 cm^{-1} (Figure 3a). The D/G intensity ratio in graphitic materials has

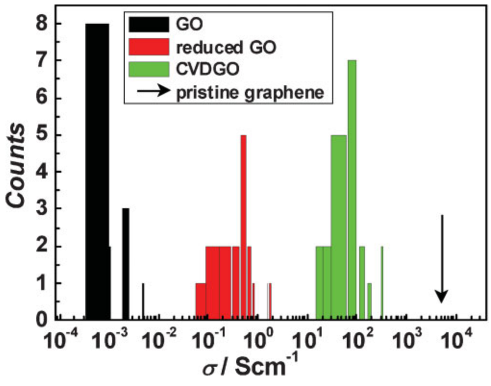

Figure 1. Histogram of the experimentally determined electrical conductivity distribution for monolayers of GO, reduced GO and CVDGO. The conductivity of pristine graphene, as reported in the literature [3], has been added for comparison.

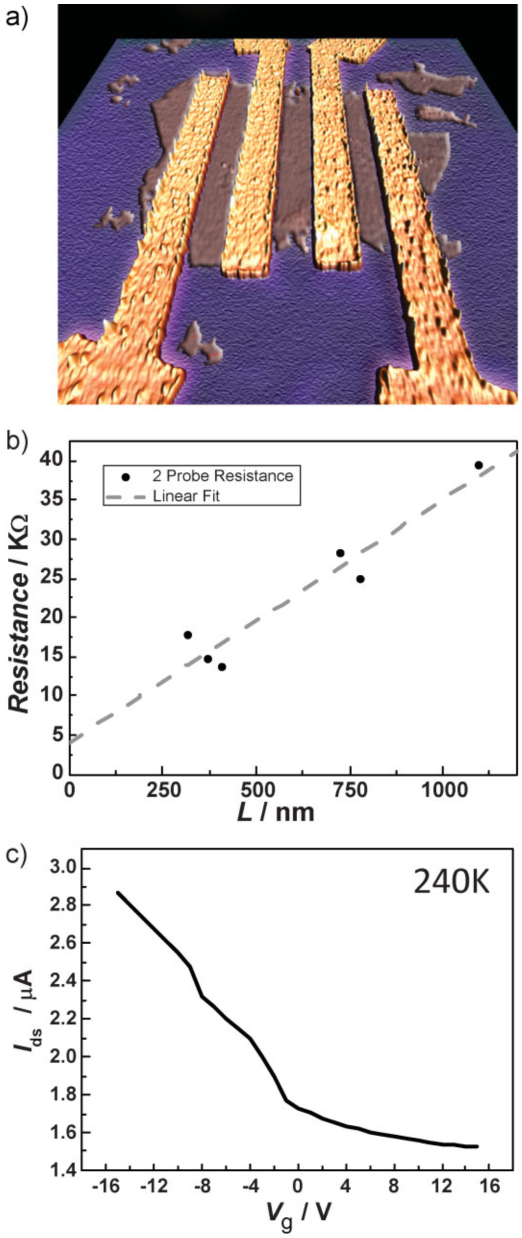

Figure 2. a) AFM image of a four-probe CVDGO single-layer device. The scale bar is 1 µm. b) Room-temperature two-probe resistance as a function of channel length measured on the device in the upper panel. The resistance increases linearly with channel length with an intercept at 4 kΩ indicative of the contact resistance. c) Drain–source current as a function of back gate voltage for a device measured at 240 K under a low pressure of helium.

been used according to the Tuinstra–Koenig relation as a measure for the size of sp^2-domains,[22] based upon the assumption that the G-line scales with the domain area and thus grows with its radius r^2, whereas its defect-containing circumference changes as r. Interestingly, the D/G ratio in CVDGO is found to be larger than for chemically reduced GO[11] and, furthermore, the CVDGO exhibits an approximately linear rise of electrical conductivity with increasing D/G ratio (Figure 3b), a trend that appears counterintuitive on first impression. One possible reason for these features is the deposition of amorphous carbon onto the substrate during the CVD process. However, this scenario can be excluded in view of the essentially preserved AFM height and area[23] of the sheets, as well as the fact that no carbon-related Raman signal could be detected upon examination of the Si/SiO_2 substrate background. An alternative, reasonable explanation draws upon the above-mentioned model underlying the Tuinstra–Koenig relation, namely the creation of small patches of graphene within holes of the reduced GO[24,25] simultaneously with carbon replacement during the CVD step. The small size of these holes is expected to restrict the size of the new graphene islands to just a few nanometers, and to enhance the probability that they assume a certain mismatch with respect to the surrounding graphene lattice. On this basis, the increased D/G ratio emerges as a direct consequence of the increased number of smaller nascent regions.

The creation of additional graphene-like domains is supported by temperature-dependent electrical measurements. The CVDGO monolayers display a decrease in conductivity by more than one order of magnitude upon cooling from room temperature to 4 K, in contrast to exfoliated graphene that exhibits a conductivity decrease with increasing temperature due to the reduced mean free path caused by electron–phonon scattering.[26] This difference provides evidence that the electrical transport mechanism in these samples is, despite the significant higher conductivity, more akin to chemically reduced GO. In fact, the temperature dependence of the measured source–drain current (see Fig. 4) fits well to the following relation describing two-dimensional variable-range hopping (the first term) in parallel with electric field-driven tunneling[27] (the second term):

$$I(T) = I_1 \exp\left(-\frac{B}{T^{1/3}}\right) + I_0 \qquad (1)$$

where T is the temperature and B the hopping parameter, defined as:

$$B = \left(\frac{3}{k_B N(E_F) L_l^2}\right) \qquad (2)$$

where k_B is Boltzmann's constant, $N(E_F)$ the density of mobile carriers and L_l the localization length. For this transport mechanism, the tunneling term (I_0) becomes the dominant

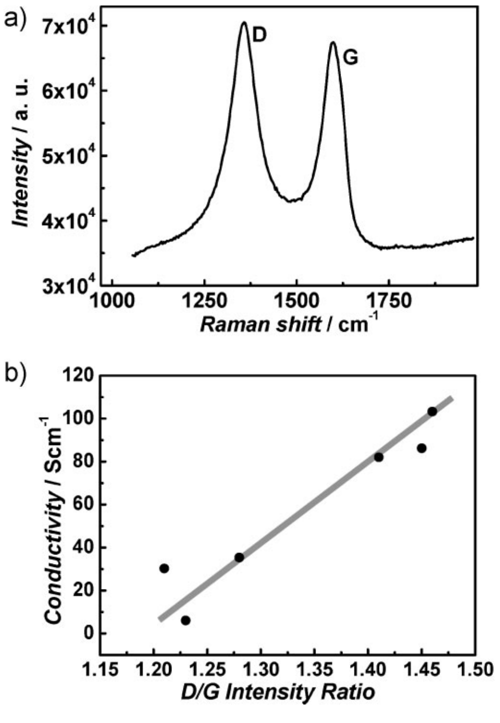

Figure 3. a) Representative Raman spectrum of a CVDGO monolayer displaying a D/G ratio larger than 1. b) Plot of conductivity vs. D/G intensity ratio displaying a monotonic rise with conductivity.

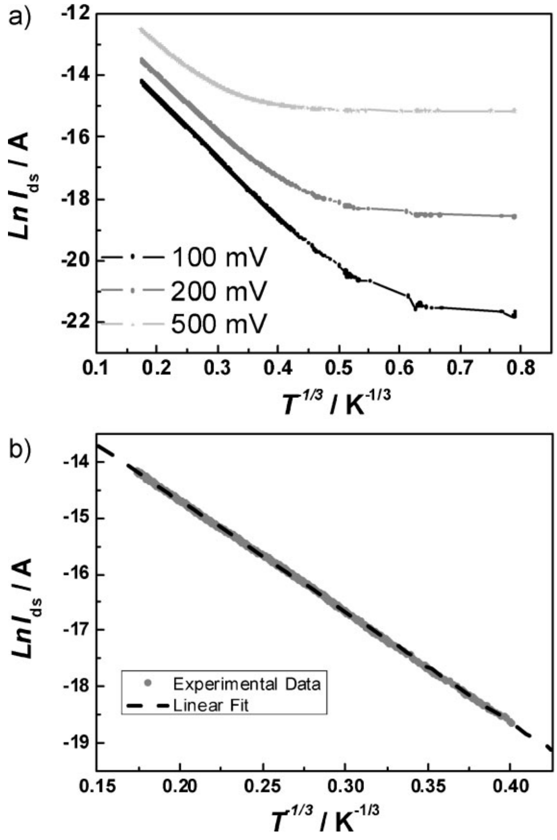

Figure 4. Plot of drain–source current (I_{ds}) against $T^{-1/3}$ at different V_{ds} applied to a CVDGO monolayer. Two regimes of conduction are observed. b) Magnified view of the hopping regime at low bias (100 mV). A two-dimensional variable range hopping model shows a perfect linear fit, indicating the presence of charge transport barriers due to defects.

contribution at lower temperatures and high electric fields. Compared to chemically reduced GO monolayers,[27] the CVDGO sheets exhibit a lower slope in the $\ln(I/A)$ vs. $T^{-1/3}$ plots, implying either a larger localization length, L_l, or a larger density of mobile carriers, $N(E_F)$. Both cases are consistent with the creation of new nanometer-sized sp^2 islands, as these would contribute more mobile charges and also enhance carrier delocalization due to the diminishment of the defect areas.

In conclusion, we have demonstrated that highly conductive chemically derived graphene is accessible through CVD-based defect healing in reduced graphene oxide. The obtained material displays, despite its significant content of residual defects, a mobility exceeding that of the molecular semiconductors currently used in organic electronics. The contained defects may be exploited as suitable anchor sites for chemical functionalization[28] or may confer ferromagnetic properties to the layers.[29,30] Moreover, the easy up-scalability of the two-step process could establish chemically derived graphene as the major component of a wide range of flexible, low-cost electronic devices. Finally, the very active current research on the CVD synthesis of carbon nanostructures[31] could act as a driving force to successfully grow more extended sp^2 regions inside the sheets, and hence further approach the electrical performance of pristine graphene.

Acknowledgements

V. L. and R. S. S. contributed equally to this work. The authors would like to acknowledge Alan Kaiser for fruitful discussions. The support of the Spanish Ministerio de Educación y Ciencia (nos. MAT2007-66476-C01/02 and NAN2004-09183-C10-05/06), CAM (no. S-0505/MAT/0303) and the European Union (no. FP6-029192) is gratefully acknowledged.

Received: May 12, 2009
Revised: June 9, 2009
Published online: August 31, 2009

[1] X. Du, I. Skachko, A. Barker, E. Y. Andrei, *Nat. Nanotechnol.* **2008**, *3*, 491.
[2] J. H. Chen, C. Jang, S. D. Xiao, M. Ishigami, M. S. Fuhrer, *Nat. Nanotechnol.* **2008**, *3*, 206.
[3] K. S. Novoselov, A. K. Geim, S. V. Morozov, D. Jiang, Y. Zhang, S. V. Dubonos, I. V. Grigorieva, A. A. Firsov, *Science* **2004**, *306*, 666.
[4] K. S. Novoselov, D. Jiang, F. Schedin, T. J. Booth, V. V. Khotkevich, S. V. Morozov, A. K. Geim, *Proc. Natl. Acad. Sci. USA* **2005**, *102*, 10451.
[5] C. Berger, Z. M. Song, T. B. Li, X. B. Li, A. Y. Ogbazghi, R. Feng, Z. T. Dai, A. N. Marchenkov, E. H. Conrad, P. N. First, W. A. de Heer, *J. Phys. Chem. B* **2004**, *108*, 19912.
[6] K. S. Kim, Y. Zhao, H. Jang, S. Y. Lee, J. M. Kim, J. H. Ahn, P. Kim, J. Y. Choi, B. H. Hong, *Nature* **2009**, *457*, 706.
[7] Z. Wei, D. E. Barlow, P. E. Sheehan, *Nano Lett.* **2008**, *8*, 3141.
[8] X. L. Li, G. Y. Zhang, X. D. Bai, X. M. Sun, X. R. Wang, E. Wang, H. J. Dai, *Nat. Nanotechnol.* **2008**, *3*, 538.
[9] Y. Hernandez, V. Nicolosi, M. Lotya, F. M. Blighe, Z. Y. Sun, S. De, I. T. McGovern, B. Holland, M. Byrne, Y. K. Gun'ko, J. J. Boland, P. Niraj, G. Duesberg, S. Krishnamurthy, R. Goodhue, J. Hutchison, V. Scardaci, A. C. Ferrari, J. N. Coleman, *Nat. Nanotechnol.* **2008**, *3*, 563.
[10] S. Stankovich, D. A. Dikin, G. H. B. Dommett, K. M. Kohlhaas, E. J. Zimney, E. A. Stach, R. D. Piner, S. T. Nguyen, R. S. Ruoff, *Nature* **2006**, *442*, 282.
[11] C. Gomez-Navarro, R. T. Weitz, A. M. Bittner, M. Scolari, A. Mews, M. Burghard, K. Kern, *Nano Lett.* **2007**, *7*, 3499.
[12] S. Gilje, S. Han, W. Minsheng, L. W. Kang, R. B. Kaner, *Nano Lett.* **2007**, *7*, 3394.
[13] I. Jung, D. A. Dikin, R. D. Piner, R. S. Ruoff, *Nano Lett.* **2008**, *8*, 4283.
[14] D. Li, M. B. Muller, S. Gilje, R. B. Kaner, G. G. Wallace, *Nat. Nanotechnol.* **2008**, *3*, 101.
[15] G. Eda, G. Fanchini, M. Chhowalla, *Nat. Nanotechnol.* **2008**, *3*, 270.
[16] X. Wang, L. J. Zhi, K. Mullen, *Nano Lett.* **2008**, *8*, 323.
[17] H. A. Becerril, J. Mao, Z. Liu, R. M. Stoltenberg, Z. Bao, Y. Chen, *ACS Nano* **2008**, *2*, 463.
[18] W. S. Hummers, R. E. Offeman, *J. Am. Chem. Soc.* **1958**, *80*, 1339.
[19] J. Kong, H. T. Soh, A. M. Cassell, C. F. Quate, H. J. Dai, *Nature* **1998**, *395*, 878.
[20] F. Schedin, A. K. Geim, S. V. Morozov, E. W. Hill, P. Blake, M. I. Katsnelson, K. S. Novoselov, *Nat. Mater.* **2007**, *6*, 652.
[21] V. Tung, M. J. Allen, Y. Yang, R. B. Kaner, *Nat. Nanotechnol.* **2009**, *4*, 25.
[22] A. C. Ferrari, J. Robertson, *Phys. Rev. B* **2000**, *61*, 14095.
[23] I. Horcas, R. Fernandez, J. M. Gomez-Rodriguez, J. Colchero, J. Gomez-Herrero, A. M. Baro, *Rev. Sci. Instrum.* **2007**, *78*.
[24] A. Lerf, H. Y. He, M. Forster, J. Klinowski, *J. Phys. Chem. B* **1998**, *102*, 4477.
[25] W. W. Cai, R. D. Piner, F. J. Stadermann, S. Park, M. A. Shaibat, Y. Ishii, D. X. Yang, A. Velamakanni, S. J. An, M. Stoller, J. H. An, D. M. Chen, R. S. Ruoff, *Science* **2008**, *321*, 1815.
[26] K. I. Bolotin, K. J. Sikes, J. Hone, H. L. Stormer, P. Kim, *Phys. Rev. Lett.* **2008**, *101*.
[27] A. B. Kaiser, C. Gómez-Navarro, R. S. Sundaram, M. Burghard, K. Kern, *Nano Lett.* **2009**, *9*, 1787.
[28] R. S. Sundaram, C. Gomez-Navarro, K. Balasubranianian, M. Burghard, K. Kern, *Adv. Mater.* **2008**, *20*, 3050.
[29] J. Fernandez-Rossier, J. J. Palacios, *Phys. Rev. Lett.* **2007**, *99*, 177204.
[30] Y. Wang, Y. Huang, Y. Song, Z. Xiaoyan, Y. MA, J. Liang, C. Yongsheng, *Nano Lett.* **2009**, *9*, 220.
[31] C. Liang, Z. Li, S. Dai, *Angew. Chem. Int. Ed.* **2008**, *47*, 3696.